J Sol-Gel Sci Technol (2013) 66:68–72
DOI 10.1007/s10971-013-2968-y

ORIGINAL PAPER

Synthesis of titanium dioxide nano-powder via sol–gel method at ambient temperature

Milad Dalvandi · Behrouz Ghasemi

Received: 27 October 2012 / Accepted: 18 January 2013 / Published online: 30 January 2013

Abstract Titanium dioxide is a semiconductor with excellent photo catalytic properties and an important material with high regarded in nanotechnology. In this study, titanium dioxide nanoparticles was successfully synthesized via sol–gel method using tetra-n-butyl orthotitanate, hydrochloric acid and ammonia. Tetra-n-butyl orthotitanate was used as precursor. The ingredients were mixed at ambient temperature for 9 h on a magnetic stirring, sol was formed and converted to gel by adding ammonia. X-ray diffraction analysis clearly showed anatase and rutile phases so that, with increasing calcination temperature anatase converts to the rutile. Scanning electron microscopy was used for agglomerate observations. Energy-dispersive detector analysis was carried out and confirmed the formation of titanium dioxide. The influences of calcination temperature and pH value on particles size were studied. The results indicate that synthesis at room temperature reduced the particle size to 15 nm.

Keywords Sol–gel · Titanium dioxide · Calcinations

1 Introduction

In recent years much attention has been paid to the preparation of one-dimensional (1D) nanomaterials, such as nanofibers, nanowires, nanorods, nanotubes, and nanobelts, which exhibit novel physical and chemical properties due to their unique characteristics for huge ratio of diameter to length, superior mechanical toughness, and so on. Due to its unique properties, titanium dioxide belongs to the group of the most attractive nanomaterials and recently possesses a great attention. TiO_2 is a n-type dielectric and its energy gap is about 3.1 eV and its refractive index is 2.6. TiO_2 powders possess interesting optical, dielectrical, and catalytical properties, which results in industrial applications such as gas sensors, chemical sensors, pigments, optical lasers, solar cells, fillers, catalyst supports, and photocatalysts. One of the major limits of using TiO_2 as photocatalyst is their relatively low value of overall quantum efficiencies, combined with the necessity of using near ultraviolet radiation [1–3].

Control of the size, shape, and structure of the colloidal precursor is an important factor in determining the properties of the final material. Titania powders have been obtained either directly from titanium bearing minerals or by precipitation from solutions of titanium salts or alcoxides. The effect of crystallite size and quantum size effect is observed in gaseous photocatalytic hydrogenation of acetylene with H_2O [4]. However, there are few studies on photocatalytic activity of nanoparticle TiO_2 crystallites in aqueous suspension systems [5].

There are several methods for producing nanoparticles. These methods are basically divided into three groups: Condensation of a vapor, chemical synthesis and solid-state processes. The most common procedures of TiO_2 preparation were based on the hydrolysis of acidic solutions of Ti (1 V) salts [4, 5]. In addition, gas-phase oxidation reactions of $TiCl_4$ and hydrolysis reactions of titanium alcoxides were used to generate finely separated, high purity TiO_2 powders. However, these powders have generally lacked the properties of uniform size, equated shape, and unagglomerated state desired for quantitative studies of colloidal phenomena [6]. Recently, several techniques

M. Dalvandi (✉) · B. Ghasemi
Department of Material Science and Engineering, Faculty of Material Science and Engineering, Semnan University, PO box 35131-19111, Semnan, Iran
e-mail: milad.dlv@gmail.com

were reported for synthesizing titania nanoparticles through controlled nucleation and growth processes in dilute Ti(IV) solutions such as sol–gel technique, hydrothermal method, chemical vapor deposition, direct oxidation and others. Among them, the sol–gel technique is one of the most used methods due to its possibility of deriving unique metastable structure at low reaction temperatures and excellent chemical homogeneity. In sol gel processes, TiO_2 is usually prepared by the reactions of hydrolysis and polycondensation of titanium alkoxide, $(TiOR)_n$ to form oxopolymers, which are transformed into an oxide network [7–9].

In this work, nanocrystalline anatase and rutile TiO_2 particles with crystallite size 15 nm have been derived via sol gel precipitation of alkoxides followed by calcination. The influence of calcination temperature and pH towards the development of titania nanocrystal structure and their performance as photocatalyst is investigated.

2 Experimental

In this study, tetra-n-butyl orthotitanate (CH3CH2CH2 CH2O)4Ti was considered as metal precursor and deionized water used as diluents solution. The molar ratio of tetra nbutyl orthotitanate to deionized water calculated by stoichiometry. Tetra-n-butyl orthotitanate mixed to deionized water with a ratio of 1–5. Deionized water stirred steadily with magnetic stirring, then tetra-n-butyl orthotitanate added drop wise into it using a syringe under magnetic stirring at room temperature [10]. At this stage, by adding hydrochloric acid 35 % as a catalyst, we adjusted the pH to a certain extent to achieve the sol (pH = 5). This sol was stirred for 12 h at ambient temperature, to be uniform. An addition stirring up to 48 h revealed that sol was still uniform and stable and no sediment was observed. So, chemical and physical stability of sol was proved in duration of 48 h. For transition of sol to gel, pH of a dispersion changed using ammonia solution (pH = 5). The obtained gel was milky color and completely stable and dried at 80 °C in an oven for 18 h. Afterward bulks were crumbled easily into powders and calcined at 450, 500, 550, 600, 650, 700 and 750 °C at the heating rate of 15 °C/min with a soaking time of 2 h in electric furnaces and cooled overnight to reach the final titanium dioxide powder. Then samples were milled for 3 h in a ball mill. Methanol used to prevent particles from sticking and sintering while samples were milling. Milled powders dried for 2 h to get out of methanol at a temperature of 80 °C [11, 12]. X-ray diffraction (XRD) patterns of different powders recorded between 10° and 60° (2θ). Samples were diaglomerated by soaking in an ultrasonic bath for 5 min, then shape and size of these samples observed by scanning electron microscopy (SEM). A quality of synthesis of TiO_2 samples in this experiment proved using EDS analysis.

3 Results and discussion

Most processes involve deposition of sulfate or chloride solutions which led to the synthesis of anatase, however, many practical applications need to have the rutile phase. Both anatase and rutile have photocatalytic properties, but in different degrees. In some cases, the highest photocatalytic degree of titanium dioxide is a mixture of anatase and rutile in a ratio of 70–30 which have the highest activity (commercial available Degussa P25). Simultaneously with increasing anatase activity, more absorption of visible light can be achieved by rutile. Alcoholic rinsing media speed up the conversion of anatase to rutile and reduce titanium dioxide conversion temperature from 800 to 550 °C. Acceleration of conversion kinetics and its mechanisms due rinsing media can be accepted from analyzing of temperature and time dependence of rutile [13, 14].

Figure 1 shows the XRD pattern of calcined samples at different temperatures. These patterns clearly show that the crystalline particles are calcined at these temperatures and they often have anatase structure. Conversion of anatase to the rutile starts in the range of 550–650 °C.

Change in particle size than the calcination temperature is shown in Fig. 2. Particle size has been changed as a function of calcinations temperature change, so that the particle size also increased with increasing calcinations temperature. Particles growth at low calcinations temperatures has occurred slowly and then this growth speed up at high temperatures. The particle growth rate (The rate of the increasing particle diameter) is obtained by Eq. 1 [15].

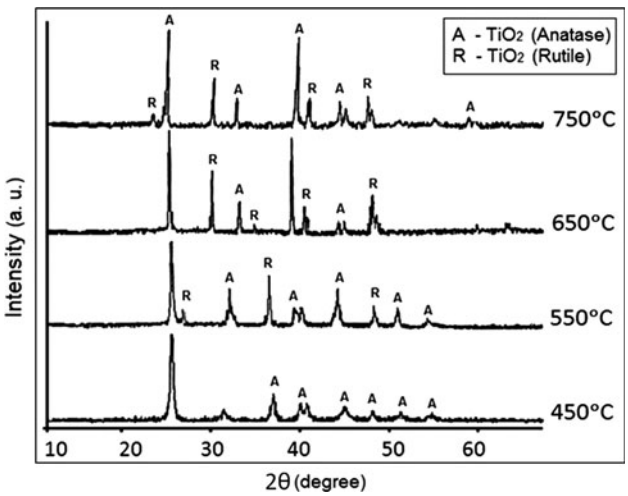

Fig. 1 XRD pattern of samples at various calcinations temperatures

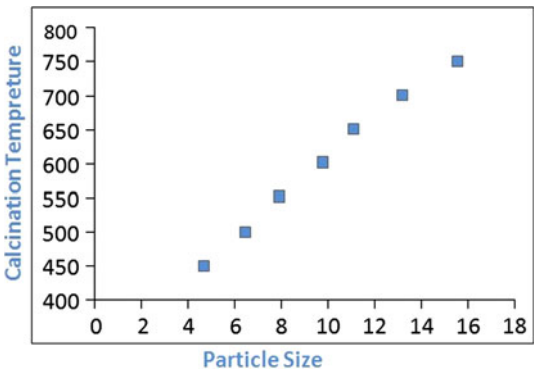

Fig. 2 Changes in particle size as a function of calcination temperature

$$V = a \cdot \upsilon \left[\exp(-Q/kT)\right]\left[1 - \exp(\Delta F\nu/kT)\right] \quad (1)$$

In this equation, a is particle diameter, U is atoms mutation frequency, Q is the activation energy of an atom that has left the network and attaches itself to the growing phase, and ΔFν is the Molar free energy difference between the two phases. For non-crystalline structures ΔFν is much greater than kT, so Eq. 1 can be modified Eq 2.

$$V = a \cdot \upsilon \left[\exp(-Q/kT)\right] \quad (2)$$

When calcinations temperature is high, the activation energy is too small, so growth rate is at a high level, thus the particle size increases very rapidly. While when calcinations temperature is low, the activation energy is too high and so growth rate will be reduced, therefore, the particle size decreases with decreasing calcinations temperature.

SEM images of titanium dioxide nanoparticles that were prepared at different calcinations temperatures can be seen in Figs 3, 4, 5, 6. Nanoparticles of titanium dioxide with dimensions less than 15 nm at a calcinations temperature of 450 °C are visible and accessible. This is clearly seen in the SEM images, and is easily recognizable. Also in SEM images we can see that with increasing in calcinations temperature particle size is relatively increased [16].

As we see, the results of the SEM images are consistent with the results of XRD (peaks breadth) and are coordinated with each other, and confirm the dependence of particle size with calcinations temperature. The particles sizes in the SEM images are shown in Figs. 4, 5, 6 (magnification of 75,000×). In this magnification synthesized powder can be clearly seen, better than at magnification of 50,000× (Fig. 3).

To ensure the accuracy of the SEM and XRD results, formation of titanium dioxide powder was fixed again (Fig. 7) by EDS analysis on samples that were studied by scanning electron microscope.

The sol–gel process is usually used to have an efficient mixture of ions at the atomic scale. In the liquid phase

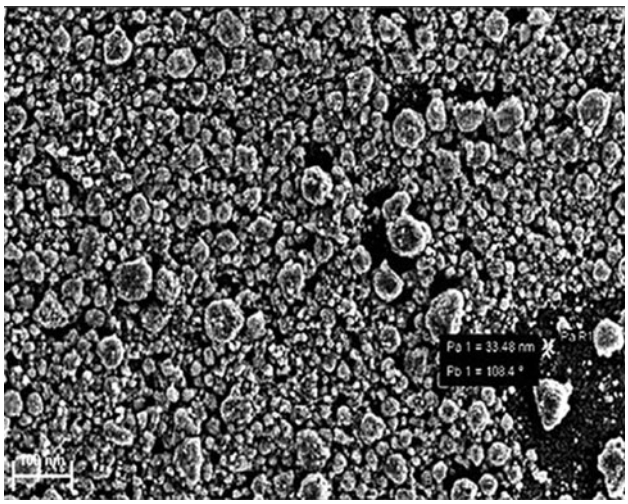

Fig. 3 SEM image of sample 1 (T-Cal: 450 °C)—×50,000)

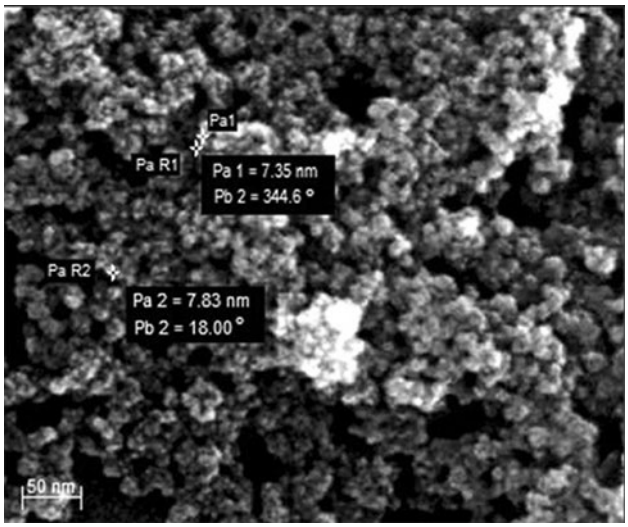

Fig. 4 SEM image of sample 3 (T-Cal: 550 °C)—×75,000)

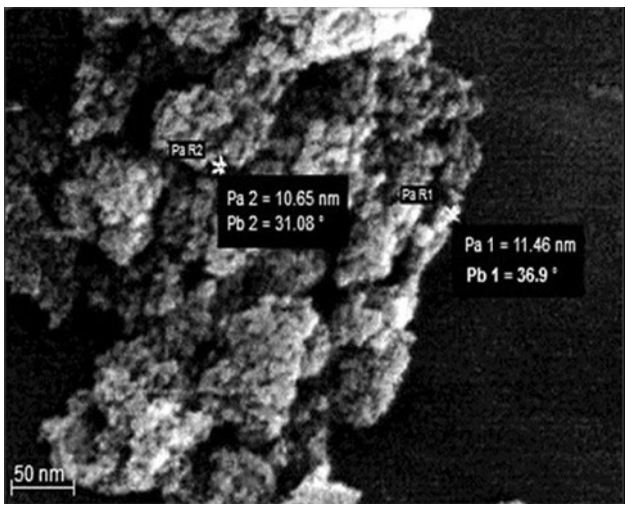

Fig. 5 SEM image of sample 5 (T-Cal: 650 °C)—×75,000

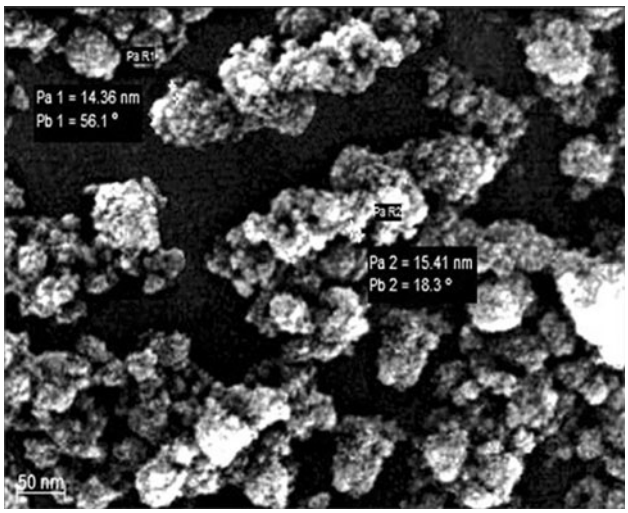

Fig. 6 SEM image of sample 7 (T-Cal: 750 °C)—×75,000

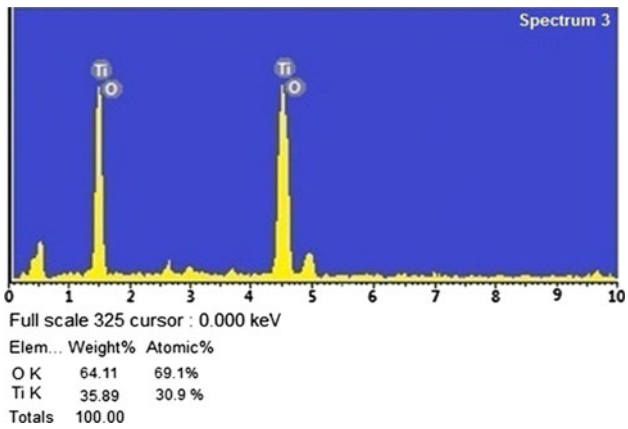

Fig. 7 EDS analysis of sample 3 (T-Cal: 550 °C)

solution, the concentration of hydrochloric acid can affect on hydrolysis reaction that can lead to the formation of many compounds. Many of organic precursor and mineral one's (metallic salts) from the point of hydrolysis view are non-stable. Hydrolysis reactions use to occur in the coordinated water molecules to metal ions because charge transfer of oxygen to metal atoms is more acidic than non-coordinated conditions. Sticking colloid particles to together and sink them in the form of larger particles, called clotting and if in converting to a semi-solid mass, it being called gel-forming type and final phase synthesis occurs during the gel formation and calcination on the acid concentration which is the changing in pH value. In this process, transmission from sol to gel, often obtained by changing the pH value or the concentration of the solution [17].

In Table 1, the crystallite size changes with respect to pH changes can be observed in the calcination temperature (650 °C). As we see, by changing the acid concentration

Table 1 Changes in crystallite size by changing the pH levels at a calcinations temperature of 650 °C)

pH	4	5	6
Crystallite size (nm)	9	14	23

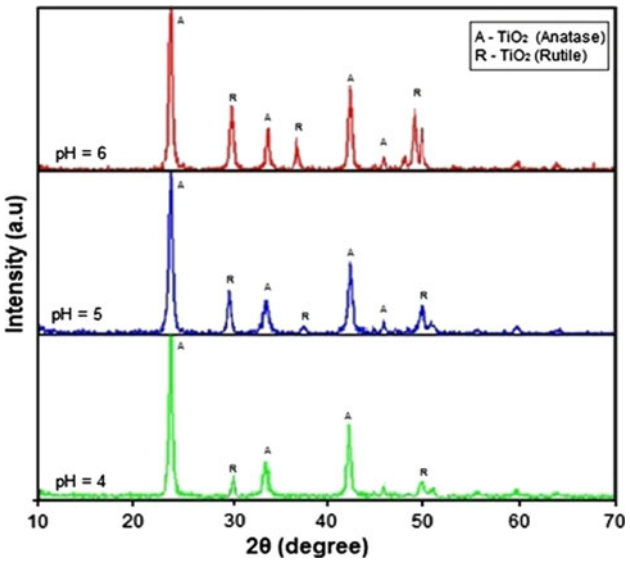

Fig. 8 XRD pattern of samples at T-calcinations 650 °C

with respect to metal cations, crystallite size will change. In Fig. 8 we observe XRD results for three different pH (for the sample with the calcination temperature of 650 °C) and also evaluation of pH changes in the phase change from anatase to rutile. We see that by increasing pH, rutile nucleation will start and with the continuing increase in mole fraction of the intensity of rutile's peaks in the XRD images also increases. Crystallite sizes given in Table 1 are calculated by the Debye-Scherer method [17].

4 Conclusion

The results showed that the titanium dioxide powder with dimensions below 15 nm by sol–gel method is reproducible. Particle size distribution in this chemical method of producing nano-powders is less evident. So that with careful control of experimental conditions we find the dimensions below 5 nm. The produced powders had spherical morphology and were almost regular, that it is due to the high chemical and physical stability of the primary sol was prepared at the beginning. Among the effective parameters on titanium dioxide particle size, the pH and its change and calcinations temperature with respect to solution concentration and calcinations time have more effect. Also calcinations times with regard to calcinations temperatures can have the same effect on particle size.

At calcinations temperatures below 550 °C the stable phase is often anatase and phase transformation from anatase to rutile which had start at 550 °C. As we observed in this study with increasing in molar fraction, we had increased in peak intensity for anatase phase in XRD patterns. By more increasing in molar fraction of acid and increasing the pH, we saw the starting of rutile nucleation and by continuing of this molar fraction increasing, intensity of rutile's peaks also increased in XRD patterns.

References

1. Brinker CJ (1990) Sol-gel science. The physics and chemistry of sol-gel processing. Academic Press
2. Wang C-C, Ying J-Y (1999) Chem Mater 11:3113–3120
3. Dr Soutar A et al Sol-gel spectrally selective coating. SIMTech Technical report
4. Bischoff BL, Anderson MA (1995) Chem Mater 7:1772–1778
5. Ding X-Z, Liu X-H (1997) J Alloy Compd 248:143–145
6. Chen X, Mao SS (2007) Chem Rev 107:2891–2959
7. Mahshid S, Sasani Ghamsari M, Askari M, Afshar N, Lahuti S (2006) Semicond Phys Quantum Electron Optoelectron 9:65–68
8. Allen NS, Edge M, Verran J, Stratton J, Maltby J, Bygott C (2008) Polym Degrad Stab 93:1632–1646
9. Bessekhouad Y, Robert D, Weber JV (2003) Int J Photoenergy 5:153–158
10. Bahnemann D, Henglein A, Spanhel L (1984) Faraday Discuss Chem Soc 78:151–163
11. Yi J, Argon AS, Sayir A (2005) J Eur Ceram Soc 25:1201–1214
12. Matson LE, Hecht NL (2005) J Eur Ceram Soc 25:1225–1241
13. Segadaes AM, Moreli MM, Akimininami RG (1997) 5th ECERs. Part I, ttp Trans. Tech. Publication, p. 209
14. Naseer YM (2005) Mater Chem Phys 94:3331
15. Henry M, Jolivet JP, Livage J (1991) In: Reisfeld R, Jorgensen CK (eds) Aqueous chemistry of metal cations, hydrolysis, condensation, and complexation. Springer, Berlin, p. 155
16. Maeda M, Watanabe T (2007) Surf Coat Tech 201:9309–9312
17. Cao F, Oskam G, Searson PC, Stipkala JM, Heimer TA, Farzad F, Meyer GJ (1995) J Phys Chem 99:11974–11980